Journal of Inflammation Research

Dovepress
Taylor & Francis Group

Open Access Full Text Article

ORIGINAL RESEARCH

Comprehensive Analysis of RNA Modifications Related Genes in the Diagnosis and Subtype Classification of Dilated Cardiomyopathy

Cuixiang Xu[1,2], Xiangrong Zhao[1,2], Huiting Li[1,2], Yaping Li[1,2], Yangmeng Feng[1,2], Guoan Zhang[3], Xiaoyan Huang[1,2]

[1]Shaanxi Provincial Key Laboratory of Infection and Immune Diseases, Shaanxi Provincial People's Hospital, Xi'an, People's Republic of China; [2]Shaanxi Engineering Research Center of Cell Immunology, Shaanxi Provincial People's Hospital, Xi'an, People's Republic of China; [3]Department of Cardiovascular Surgery, Shaanxi Provincial People's Hospital, Xi'an, People's Republic of China

Correspondence: Xiaoyan Huang, Email huangxy08@163.com

Background: RNA modifications are associated to various human diseases. However, the functions of RNA modification-related genes have yet to be thoroughly investigated in dilated cardiomyopathy (DCM). This study sought to conduct a comprehensive analysis of RNA modification-associated genes for the diagnosis and subtype classification of DCM.

Methods: We collected DCM and control sample RNA modification-related genes from Gene Expression Omnibus (GEO) microarray datasets. Differential expression analysis was performed on these using the "Limma" package in R. Univariate logistic regression, and the LASSO algorithm were used to identify optimal genes for diagnostic model establishment. Furthermore, ConsensusClusterPlus was used to identify RNA modification-molecular subtypes. Lastly, the expression of the hub RNA modification-related genes and their connection to DCM were confirmed using the clinical samples and mouse models.

Results: Twenty-six RNA modification-related genes were identified as dysregulated in DCM, with strong connections noted among these genes. A diagnostic model based on 13 genes (*TRMT61B, MBD2, YTHDC2, NOP2, TRMT10C, WDR4, CPSF2, CSTF3, ZBTB4, UNG, NSUN6, TET1*, and *DNMT3B*) with an AUC of 0.980 predicted DCM well. Infiltrating plasma B cells, eosinophils, CD8 T cells, and regulatory T cells correlated strongly with *TRMT61B, MBD2, YTHDC2*, and *CPSF2*. Two RNA modification-molecular subtypes (clusters 1 and 2) were identified. Cluster 1 had greater RNA modification scores, lower immune ratings, and lower HLA-DRB1 and HLA-DPB1 expression than Cluster 2. Cluster 2 engaged metabolism-related pathways, while Cluster 1 activated renin-angiotensin system pathways.We further found a substantial link between lower cardiac function and up-regulation of *TET1, DNMT3B*, and down-regulation of *MBD2, TRMT61B* in the 13 hub RNA modification-related genes.

Conclusion: In conclusion, our RNA modification-related diagnostic model predicts DCM well. The discovery of two RNA modification-molecular subgroups and four key pivotal genes may assist stratify DCM patients by risk.

Keywords: dilated cardiomyopathy, RNA modification, N^6-methyladenosine, 5-methylcytosine, immune infiltration

Introduction

Dilated cardiomyopathy (DCM) is a common primary cardiomyopathy marked by left ventricular (LV) dilation and systolic impairment.[1] The clinical manifestation of DCM ranges from asymptomatic conditions to heart failure, ventricular arrhythmias, and sudden cardiac death. The causes of DCM are diverse, encompassing several hereditary and non-genetic factors. Non-genetic etiologies encompass infections, autoimmune disorders, myocarditis, and exposure to alcohol, chemicals, and poisons. Genetic mutations affecting genes related to cytoskeletal, sarcomeric components, and mitochondrial and nuclear envelope proteins comprise around 30–50% of patients.[2,3] These genetic abnormalities are consistently identified during the screening and clinical diagnosis of familial DCM.[4] Patients with DCM due to non-genetic causes may potentially be affected by their genetic makeup.[5] Consequently, a comprehensive comprehension of

Received: 26 October 2024
Accepted: 13 May 2025
Published: 15 May 2025

the correlations between unique DCM phenotypic attributes and genetic and molecular traits, along with advancements in early screening, would enhance the diagnosis, prevention, and treatment of DCM.

Growing evidence has shown the correlation between DCM clinical characteristics and epigenetic regulation, alongside genetic variations.[6,7] RNA modifications are regarded as vital posttranscriptional regulators of gene expression programs, significantly influencing numerous developmental processes.[8] In recent years, RNA modifications have garnered attention due to the advent of RNA sequencing techniques for mapping modification sites, novel methods for accurate detection and quantification of modifications, and the comprehensive characterization of RNA modification effectors: "writers" "erasers" and "readers"[9].

More than 170 distinct chemical modifications have been reported on RNAs, including N6-methyladenosine (m^6A), N1-methyladenosine (m^1A), 5-methylcytosine (m^5C), N7-methylguanosine (m^7G), and alternative polyadenylation (APA) alterations. These RNA modifications are reversible and dynamic, typically facilitated by "writers" "erasers" and "readers" and play a role in different physiological and pathological processes. For instance, the m^6A demethylase FTO was downregulated in a diabetic cardiomyopathy mouse model, and its overexpression enhanced cardiac function by mitigating myocyte hypertrophy and myocardial fibrosis.[10] The m^6A "reader" protein YTHDC1 facilitates proper contractile function, and its absence leads to the onset of DCM (characterized by significant LV enlargement and severe systolic dysfunction) in mice due to the aberrant splicing of Titin (TTN).[11] Moreover, mutations in TTN are recognized to cause DCM, present in roughly 18% of sporadic instances and 25% of familial instances.[12] Levels of m6A in mRNA from human heart failure samples were found to be elevated compared to control samples.[13] Additionally, interactions may exist among these RNA modifications. For instance, the prominent m^6A "readers" YTHDF1-3 and YTHDC1 can also function as "readers" that directly attach to m^1A in RNA.[14] Nevertheless, contemporary research has predominantly concentrated on the individual genes associated with m^6A modification in DCM, with limited evidence regarding the functions of various RNA modifications in DCM as a whole.

This study conducted an integrated investigation of multiple RNA modification-related genes in DCM. Genes associated with RNA modification exhibiting unique expression patterns in DCM were analyzed, leading to the identification of biomarkers for DCM to develop a diagnostic model. Furthermore, we endeavored to categorize DCM patients into different populations exhibiting varying genetic and molecular traits based on RNA modification-related genes. Ultimately, we employed clinical data to validate the association between the hub RNA modification-related genes and DCM. This work elucidates the correlations between DCM phenotypic characteristics and epigenetic regulation.

Methods

Data Acquisition

The microarray datasets GSE141910 and GSE120895 were obtained from the Gene Expression Omnibus (GEO) database. The GSE141910 dataset served as the training set, consisting of 332 LV free-wall tissue samples from 166 non-failing healthy donors (control) and 166 DCM patients, which were collected for analysis. The data in GSE141910 was produced using the GPL16791 Illumina HiSeq 2500 platform. The GSE120895 dataset included 55 tissue samples from 47 patients with DCM and 8 persons with normal LV systolic function (controls). The data in GSE120895 was produced using the GPL570 Affymetrix Human Genome U133 Plus 2.0 Array platform. The GSE120895 dataset used as an external validation set.

RNA Modification-Related Genes

A total of 63 RNA modification-related genes were identified from prior research,[15,16] and the expression levels of these genes were extracted from the GSE141910 dataset.

Differential Expression Analysis

Differentially expressed RNA modification-related genes (DERMGs) between the DCM and control groups (CTRL) were identified using the "Limma" package with a cut-off value of FDR < 0.05. Similarly, differential expression genes

between two molecule clusters were also screened using the "Limma" package with cut-off values of FDR < 0.05 and | log2FC| > 0.263.

Function Enrichment Analyses

Enrichment analysis for biological process keywords in Gene Ontology (GO) annotations and Kyoto Encyclopedia of Genes and Genomes (KEGG) pathways was performed using DAVID (version 6.8) with a threshold of FDR < 0.05. Furthermore, pathways that were differentially enriched between two molecular clusters were examined using gene set variation analysis (GSVA). MSigDB (https://www.gsea-msigdb.org/gsea/msigdb/index.jsp), a pre-defined set of genes, used as an enrichment reference. Each pathway was measured utilizing GSVA (version 1.36.3), followed by the identification of differential pathways between two molecular clusters using an FDR < 0.05.

Establishment and Evaluation of Diagnostic Model

To identify genes linked to DCM, the DERMGs were examined using univariate logistic regression analysis provided in the "rms" package (version 6.3–0), in which DERMGs with P < 0.05 were selected. Next, the LASSO algorithm provided in the "lars" package (version 1.2) was further used to screen optimal DERMGs. Finally, a diagnostic classifier was established based on these optimal DERMGs using the Support Vector Machine (SVM) method provided in the "e1071" package (version 1.6–8). The predictive performance of the diagnostic classifier was evaluated by the receiver operator characteristic (ROC) curve, which was plotted using the "pROC" package (version 1.12.1).

Consensus Clustering Analysis

The best DERMGs were utilized to categorize 166 DCM patients into distinct molecular clusters with ConsensusClusterPlus (version 1.54.0). The RNA modification scores for each sample were quantified via GSVA (version 1.36.3) and compared among molecular clusters using the Kruskal−Wallis test.

Immune Infiltration Status

The CIBERSORT algorithm (https://cibersort.stanford.edu/index.php) was utilized to assess the proportions of 22 invading immune cells in tissue samples. The immune and stromal scores of tissue samples were inferred using the "ESTIMATE" package (http://127.0.0.1:29606/library/estimate/html/estimateScore.html).

Real-Time Quantitative PCR (RT-qPCR)

The study of our clinical samples adheres to the Declaration of Helsinki. Six myocardial samples were collected from Shaanxi Provincial People's Hospital, comprising three normal samples (Control group, CTRL) from donors without DCM, and three samples from patients diagnosed with DCM (DCM group). The Ethical Committee of Shanxi Provincial People's Hospital sanctioned this study, and the corresponding patient supplied written informed permission. Total RNA was extracted from myocardial samples with the Total RNA Kit I (Omega Bio-tec, Inc, USA). Total RNA was transcribed to cDNA on ice utilizing the PrimeScript™ RT reagent kit (TaKaRa, Dalian, China). Quantitative PCR (qPCR) was conducted with the Green PCR Master Mix System (Thermo Fisher Scientific). GAPDH served as an internal reference. qPCR was performed using an HT7900 Real-Time PCR System (Applied Biosystems). The relative fold change was assessed with the $2^{-\Delta\Delta CT}$ method. The key pivotal genes in myocardial samples from Mouse DCM model were confirmed also using q-PCR. The primer sequences employed are detailed in Supplementary Table S1.

Construction of Animal Models with DCM

Eight male C57/BL mice, six weeks old and weighing 20.24 ± 2.33 g, were acquired from the Laboratory Animal Center of Xi'an Jiaotong University in China. The mice were arbitrarily assigned to two groups: a control (CTRL) group and a DCM group. Four mice in each group. Each mouse in the DCM group received a cumulative dose of 4 mg/kg doxorubicin (DOX, Sigma, St. Louis, USA) through four consecutive intraperitoneal injections over 28 days, with an injection occurring once every seven days. The CTRL was administered injections of equivalent volumes of 0.9% saline at identical time intervals. Transthoracic echocardiography was conducted in the fifth week to assess cardiac function

during deep anesthesia with pentobarbital sodium (50 mg/kg, Sigma, USA). At the fifth week, cardiac tissue samples were obtained for q-PCR analysis, and all animals were euthanized by exposure to a high concentration of isoflurane. An echocardiography was performed before sacrifice, and body weight was documented during modeling.

Echocardiography

A dose of 30 mg/kg pentobarbital was administered intraperitoneally to anesthetize the mice. The KOLO SiliconWave 30 ultra-high-resolution ultrasound imaging instrument for small animals (Suzhou, China) was utilized for echocardiography. Utilizing long- and short-axis images of the left ventricle, the following parameters were assessed: left ventricular ejection fraction (LVEF), fractional shortening (FS), and left ventricular internal diameters during diastole (LVIDd) and systole (LVIDs). Data from three cardiac cycles were evaluated to evaluate cardiovascular function.

Correlation Between Hub Genes and LV Parameters in Echocardiography

The LV parameters (EF%, FS%, and LVIDs) were examined using the Pearson algorithm, and the findings were shown with the R package "ggplot2".

Statistical Analysis

All analyses were conducted utilizing R version 3.6.1. Correlation analysis was conducted utilizing the "cor" function (http://77.66.12.57/R-help/cor.test.html), and correlation heatmaps were generated using pheatmap (version 1.0.8). The proportions of immune cell infiltration between the DCM and CTRL groups, as well as between the two molecular clusters, were analyzed using the Kruskal−Wallis test. The Kruskal−Wallis test was employed to evaluate immune and stromal scores between two molecular clusters. The expression of co-stimulatory molecules and human leukocyte antigen (HLA) family genes between two molecular clusters was evaluated using Student's *t*-test. A *P*-value of less than 0.05 was deemed statistically significant.

Results

Expression Pattern of RNA Modification-Related Genes Changed in DCM

The primary analysis processes are displayed in Figure 1.

A differential expression analysis was performed to ascertain the expression pattern of RNA modification-related genes between DCM and CTRL samples. Of the identified genes, 26 exhibited significantly altered expression patterns in the DCM samples relative to the CTRL, with m^5C genes comprising fifty percent of this subset (Figure 2A). The expression of most genes was markedly downregulated in DCM, including the m^6A genes *YTHDC2, YTHDF3*, and *CBLL1*. In contrast, seven genes were markedly upregulated in DCM, including two APA genes (*PABPN1* and *CSTF3*) and five m^5C genes (*DNMT3B, TET1, NSUN6, UNG* and *ZBTB4*). A correlation heatmap indicated that the expression of the m^5C gene ZBTB38 was positively correlated with the APA genes *PCF11* and *CPSF2* but negatively correlated with the APA gene PABPN1. Such correlations were also observed for the m^6A genes *YTHDC2* and *YTHDF3*. Moreover, the expression of the m^6A genes *YTHDC2, YTHDF3*, and *CBLL1* showed a strong positive correlation with the m^5C genes *ZBTB38* and *ZBTB33* (Figure 2B). These DERMGs were significantly enriched in mRNA methylation, mRNA polyadenylation, the C-5 methylation of cytosine, and the mRNA surveillance pathway (Figure 2C and D).

RNA Modification-Related Genes-Based Diagnostic Model

A univariate logistic regression analysis was conducted on 26 DERMGs to identify genes associated with DCM, all of which shown substantial correlations with the condition (Figure 3A). LASSO analysis was further conducted to identify the most valuable genes, and an optimal gene signature with 13 DERMGs was ultimately determined (Figure 3B). Among these, the expression of *TRMT61B, MBD2, YTHDC2, NOP2, TRMT10C, WDR4*, and *CPSF2* were found to decrease in DCM, while the expression of *CSTF3, ZBTB4, UNG, NSUN6, TET1*, and *DNMT3B* were increased in DCM (Figure 3C). An SVM diagnostic classifier was then developed utilizing these 13 genes. The ROC curve demonstrated that this gene profile exhibited strong predictive performance for DCM, with an area under the curve (AUC) of 0.980

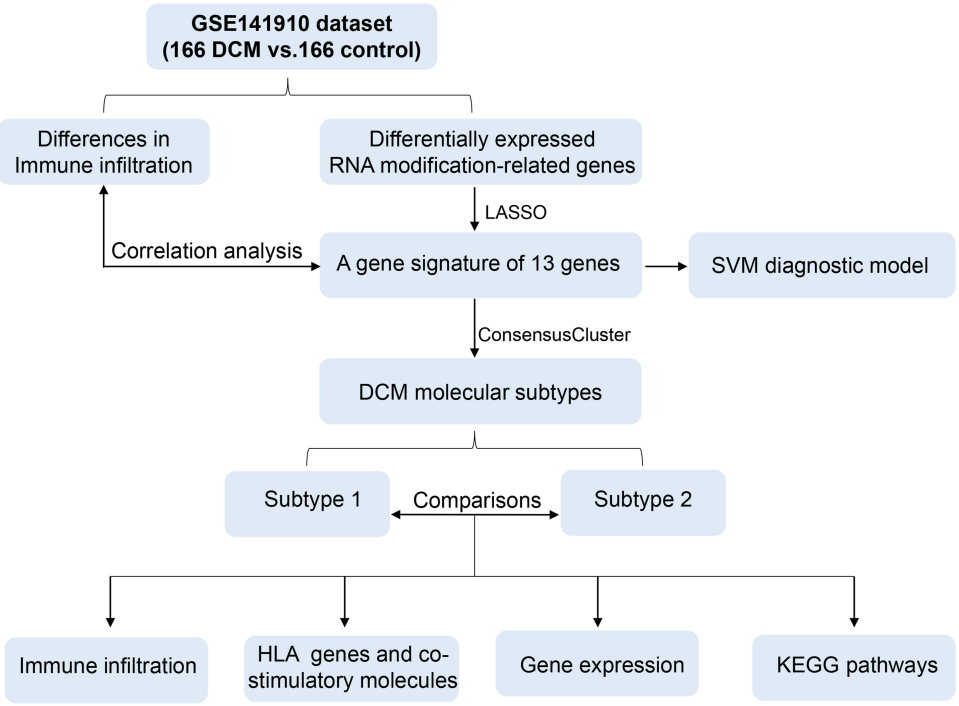

Figure 1 The workflow of this study.

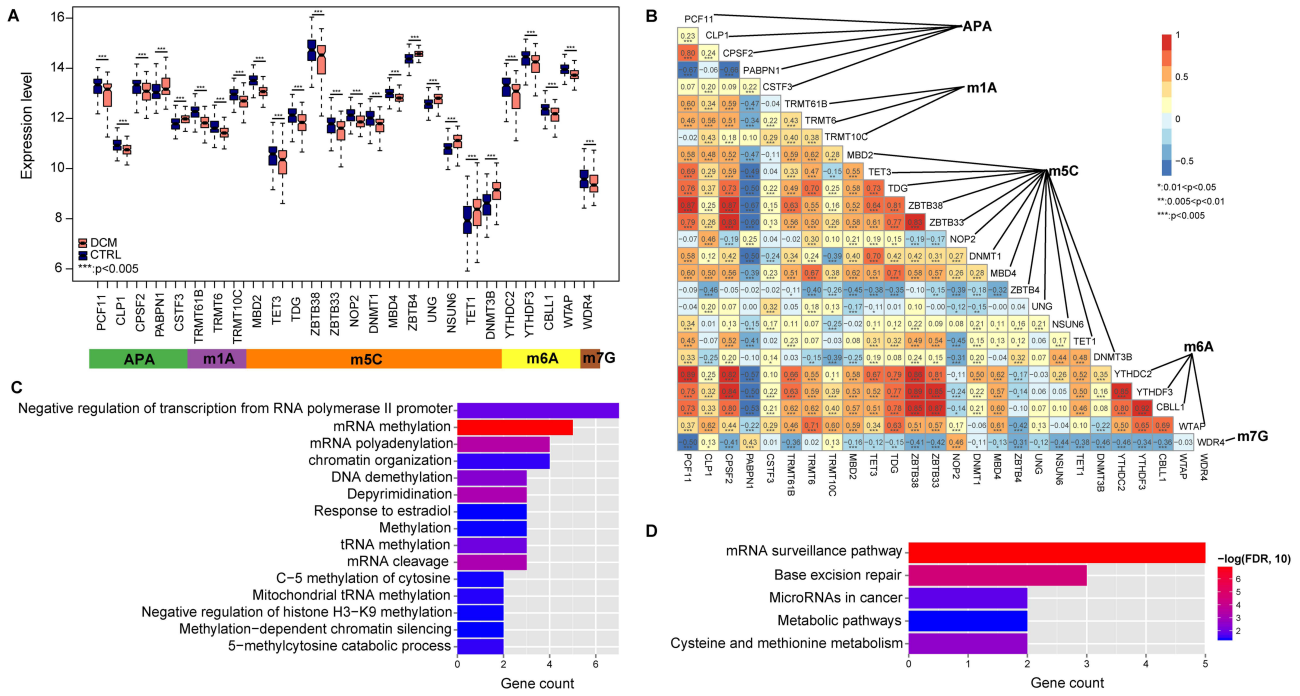

Figure 2 RNA modification-related genes in dilated cardiomyopathy. (**A**) Boxplot showing the expression levels of differentially expressed RNA modification-related genes in dilated cardiomyopathy (DCM) vs Control. (**B**) Correlation heatmap showing the correlations among the 26 differentially expressed RNA modification-related genes; The significantly enriched biological processes (**C**) and KEGG pathways (**D**) for differentially expressed RNA modification-related genes. Compared with CTRL group, 0.01<*P<0.05, 0.005<**P<0.01, ***$P<0.005$.

https://doi.org/10.2147/JIR.S498496

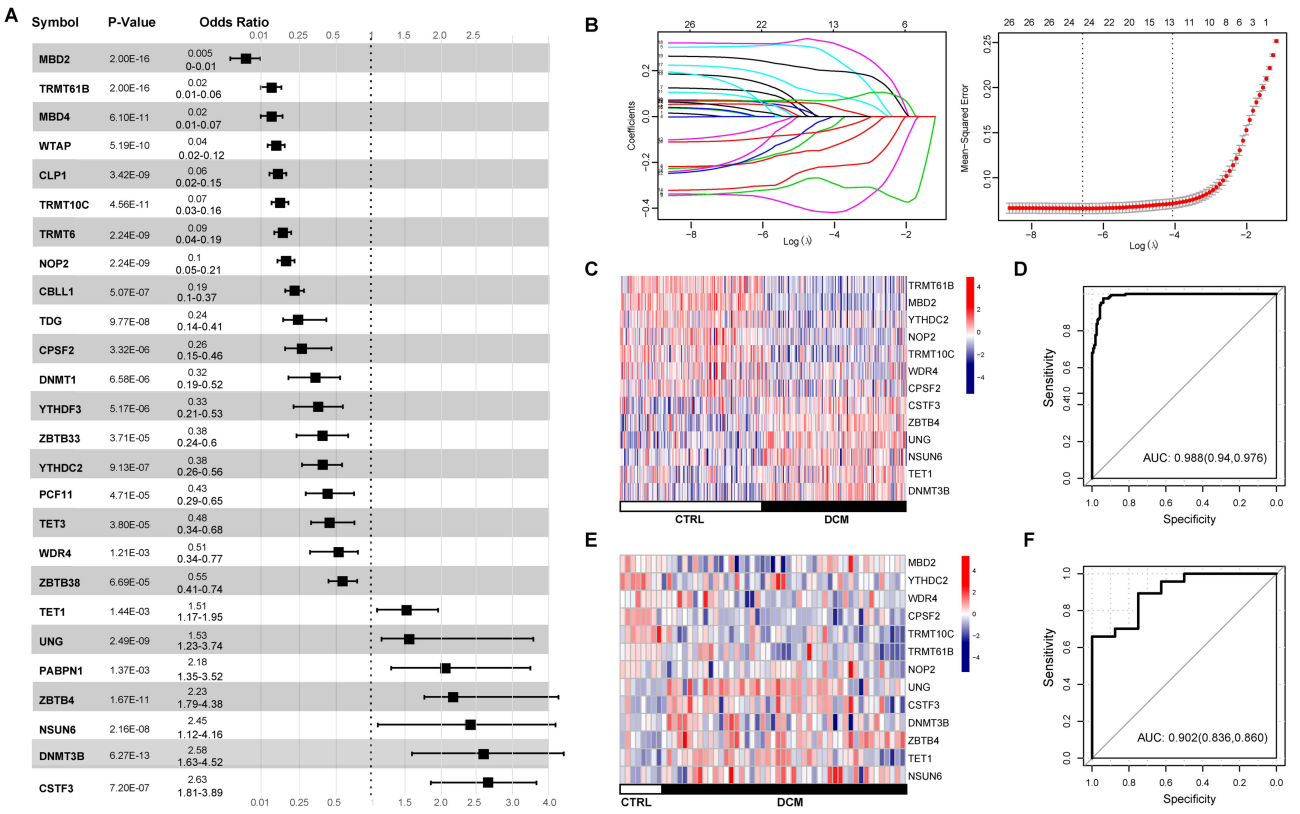

Figure 3 RNA modification-related genes-based diagnostic model. (**A**) Forest plot showing the 26 differentially expressed RNA modification-related genes significantly associated with dilated cardiomyopathy in univariate Cox regression analysis. (**B**) LASSO coefficient distribution of RNA modification-related genes and 10-fold cross-validated likelihood deviance of the LASSO coefficient for parameter selection. (**C**) Heatmap showing the expression pattern of 13 optimal diagnostic genes in GSE141910 dataset. (**D**) ROC curve showing the diagnostic performance of the diagnostic model. (**E**) Heatmap showing the expression pattern of 13 optimal diagnostic genes in GSE120895 dataset. (**F**) ROC curve showing the diagnostic performance of the diagnostic model.

(Figure 3D). The efficacy of our diagnostic classifier was corroborated using an external dataset, GSE120895, which demonstrated commendable prediction ability for DCM, yielding an AUC of 0.902 (Figure 3E–F).

Immune Infiltration Status of Left Ventricular Tissue in DCM Differed from the Control

The state of immunological infiltration was assessed utilizing CIBERSORT. Among 22 immune cell types, naive B cells, plasma B cells, resting memory $CD4^+$ T cells, M2 macrophages, and activated mast cells exhibited a comparatively significant infiltration fraction in the left ventricular free-wall tissue. Furthermore, 11 immune cells exhibited notable disparities in infiltration quantity between the DCM and CTRL samples. DCM samples exhibited a significantly elevated presence of naive B cells, M1 macrophages, activated mast cells, and neutrophils in comparison to the CTRL samples (Figure 4A). We subsequently examined the associations of the 13 optimum diagnostic genes with invading immune cells that varied between the DCM and CTRL groups. The expression levels of *TRMT61B, MBD2, YTHDC2*, and *CPSF2* exhibited a robust positive connection with the infiltration abundance of plasma B cells and eosinophils. It remained adversely linked with the amount of infiltrating CD8 T cells and regulatory T cells (Tregs) (Figure 4B).

RNA Modification-Related Genes-Based Molecule Clusters in DCM

Given the significance of the 13 optimum diagnostic genes in DCM, a consensus clustering analysis was performed based on the expression of these genes, categorizing 166 DCM patients into two molecular clusters: 116 samples in Cluster 1 and 50 samples in Cluster 2 (Figure 5A). Cluster 1 exhibited a markedly elevated RNA modification score compared to Cluster 2 (Figure 5B). The immune infiltration state varied between the two molecular clusters. Cluster 1 exhibited

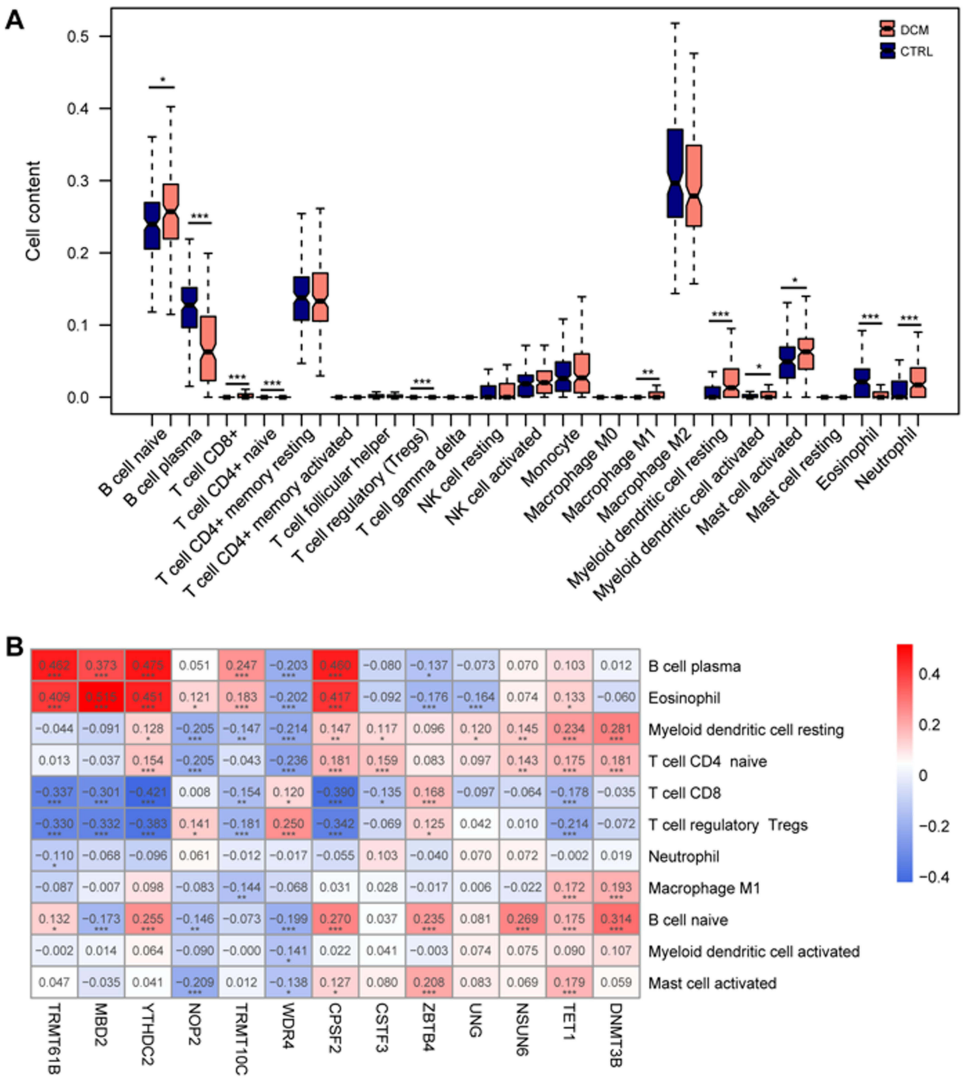

Figure 4 Associations of RNA modification-related genes with immune infiltration. (**A**) Boxplot showing the difference in infiltration abundance of 22 immune cells between dilated cardiomyopathy (DCM) and control samples; (**B**) Correlation heatmap showing the correlations between RNA modification-related genes expression and infiltration abundance of differential immune cells. Compared with CTRL group, 0.01<*P<0.05, 0.005<**P<0.01, ***$P<0.005$.

a markedly elevated stromal score (Figure 5C) and a significantly low immune score (Figure 5D) compared to Cluster 2. A total of 14 immune cells showed significant differences between Cluster 1 and 2 (Figure 5E).

Cluster 1 exhibited a greater infiltrating abundance of naive B cells, plasma B cells, and resting memory $CD4^+$ T cells, whereas Cluster 2 demonstrated a larger infiltrating abundance of M2 macrophages and monocytes. Furthermore, these two molecular clusters exhibited distinct expression patterns for HLA family genes (Figure 6A) and several co-stimulatory molecules (Figure 6B). For example, multiple HLA genes (HLA-DRB1, HLA-DPB1, and HLA-C) were highly expressed in Cluster 2 compared to Cluster 1.

Gene Expression Patterns and Pathways Between Two Clusters

To validate the two molecular clusters associated with RNA modification-related genes, their respective gene expression patterns and pathways were subsequently examined. As anticipated, the two clusters of molecules associated with RNA modification exhibited significantly distinct gene expression patterns, encompassing 742 differently expressed genes (Figure 7A and B). These genes were primarily associated with the inflammatory response, ion transmembrane transport mechanisms (such as chloride and sodium ions), neuroactive ligand-receptor interactions, and calcium signaling pathways

https://doi.org/10.2147/JIR.S498496

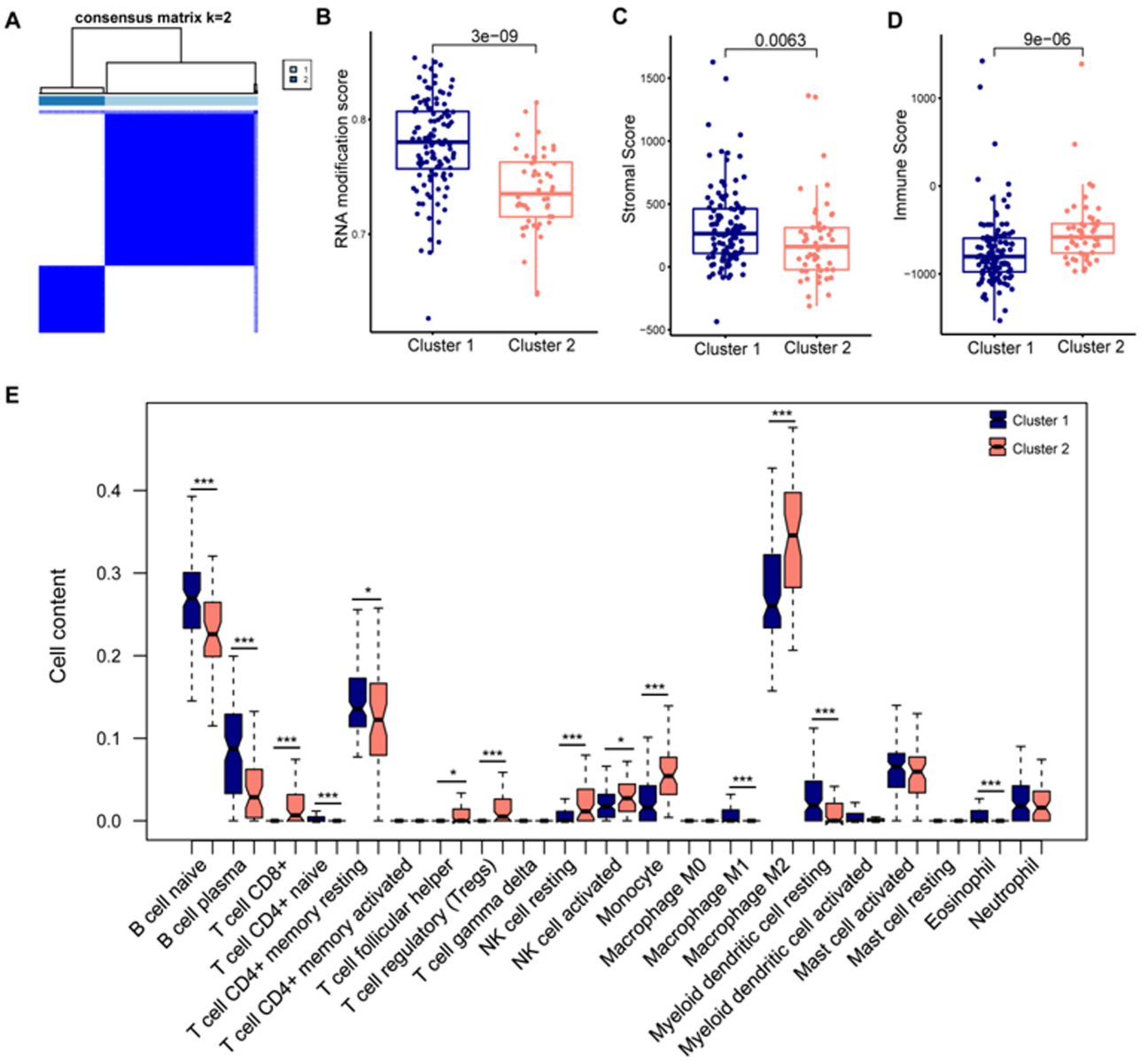

Figure 5 Consensus clustering analysis. (**A**) Consensus clustering grouped dilated cardiomyopathy samples into two clusters based on expression of RNA modification-related genes; Boxplots showing the difference in RNA modification score (**B**), stromal score (**C**) and immune score (**D**) between two clusters; (**E**) Boxplot showing the difference in infiltration abundance of 22 immune cells between two clusters. Compared with Cluster 1 group, 0.01<*P<0.05, ***$P<0.005$.

(Figure 7C and D). Additionally, GSVA identified many pathways that were differentially enriched between the two molecular clusters. Cluster 2 exhibited considerable activation of various metabolism-related pathways, including those for arachidonic acid, pyrimidine, glutathione, glycine, serine, and threonine metabolism. Conversely, primary immunodeficiency, the renin-angiotensin system, and neuroactive ligand-receptor interaction pathways were activated in Cluster 1 (Figure 7E).

Q-PCR Validated the Relationship of 13 RNA Modification-Related Genes' Levels Between Control and DCM

RT-qPCR results indicated that, in comparison to the CTRL group, the expression levels of six optimal RNA modification-related genes (*CSTF3, ZBTB4, UNG, NSUN6, TET1* and *DNMT3B*) among the 13 optimal genes were considerably elevated in the DCM group (P<0.05). The seven optimum genes (*TRMT61B, MBD2, YTHDC2, NOP2, TRMT10C, WDR4* and *CPSF2*) in the DCM group were significantly downregulated (P<0.05). *TET1, DNMT3B, MBD2* and *TRMT61B* exhibited the

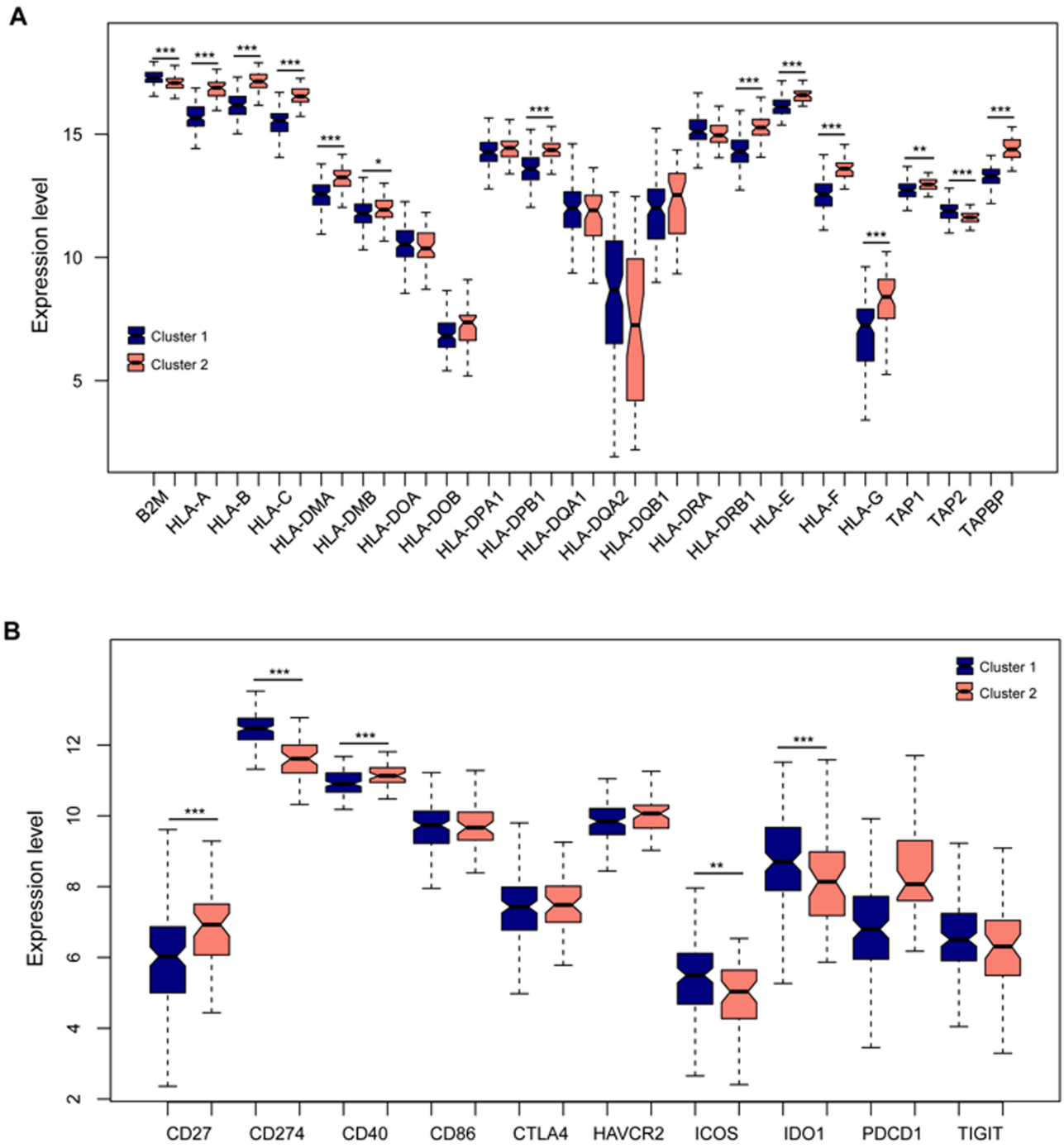

Figure 6 Expression of HLA family genes and co-stimulatory molecules. Boxplots showing the difference in expression of HLA family genes (**A**) and co-stimulatory molecules (**B**) between two clusters. Compared with Cluster 1 group, 0.01<*P<0.05, 0.005<**P<0.01, ***$P<0.005$.

most pronounced variations between the two groups (P<0.01) (Figure 8). Consequently, the subsequent murine DCM model was employed to ascertain the correlation between the four genes (*TET1, DNMT3B, MBD2*, and *TRMT61B*) and cardiac function in DCM. The validation outcomes affirmed the dependability of this diagnostic paradigm.

Experimental Validations Of four Hub Genes Expression in DCM Mice

In the modeling phase, the DCM group exhibited significantly reduced body weight compared to the CTRL group (P<0.05) (Figure 9A). The qPCR analysis of cardiac tissue samples revealed increased mRNA expression levels of *TET1*

https://doi.org/10.2147/JIR.S498496

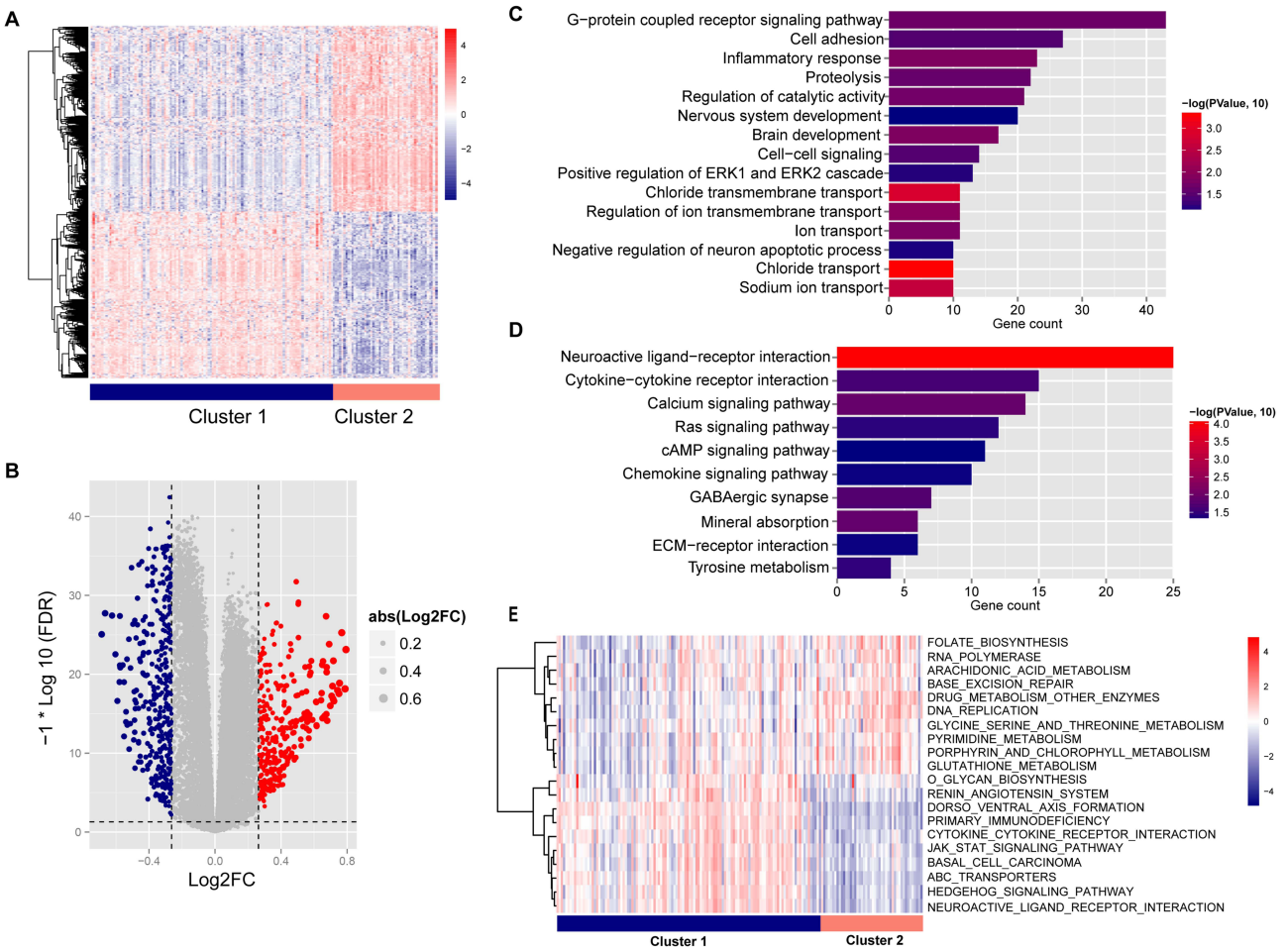

Figure 7 Gene expression and pathways between two clusters. Heatmap (**A**) and volcano plot (**B**) showing the different expression pattern of genes between two clusters; Bar charts showing the significantly enriched biological process (**C**) and KEGG pathways (**D**) for differentially expressed genes; (**E**) The pathways differentially enriched between two clusters in gene set variation analysis.

and *DNMT3B*, alongside decreased mRNA expression levels of *MBD2* and *TRMT61B* ($P<0.05$) (Figure 9C). Echocardiography demonstrated a reduction in EF% and FS% ($P < 0.05$) in the DCM group relative to the CTRL group, alongside a significantly elevated LVIDs ($P < 0.05$) (Figure 9B and D). We investigated the correlation between cardiac function and four hub genes (*TET1, DNMT3B, MBD2* and *TRMT61B*). The number of TET1 PCR cycles correlated positively with EF% ($R = 0.8891$, $P = 0.0031$) and FS% ($R = 0.8707$, $P = 0.0007$) but negatively with LVIDs ($R = -0.8756$, $P = 0.0006$). The number of DNMT3B PCR cycles correlated positively with EF% ($R = 0.8883$, $P=0.0032$) and FS% ($R = 0.8384$, $P= 0.0093$) and negatively with LVIDs ($R = -0.7506$, $P = 0.0319$). The number of *MBD2* PCR cycles correlated negatively with EF% ($R = -0.9715$, $P < 0.0001$), FS% ($R = -0.9405$, $P = 0.0005$), and positively with LVIDs ($R = 0.9328$, $P = 0.0007$). The number of *TRMT61B* PCR cycles correlated negatively with EF% ($R = -0.9527$, $P = 0.0003$), FS% ($R = -0.9664$, $P < 0.0001$), and positively with LVIDs ($R = 0.9511$, $P = 0.0003$) (Figure 9E).

Discussion

Despite growing data indicating the role of RNA modifications in various human diseases, pertinent studies on DCM are still absent. This study revealed that several RNA modification-related genes were dysregulated in DCM, including m^5C regulators. The bulk of the dysregulated genes, including m^6A regulators, were significantly down-regulated in DCM. Research has shown that m^6A alteration is essential for cardiomyocyte contractile performance and cardiac remodeling, both of which are vital in heart failure resulting from DCM.[17,18] This validated the deregulation of m^6A regulators in DCM. However, fewer research have reported on the role of m^5C regulators and other RNA

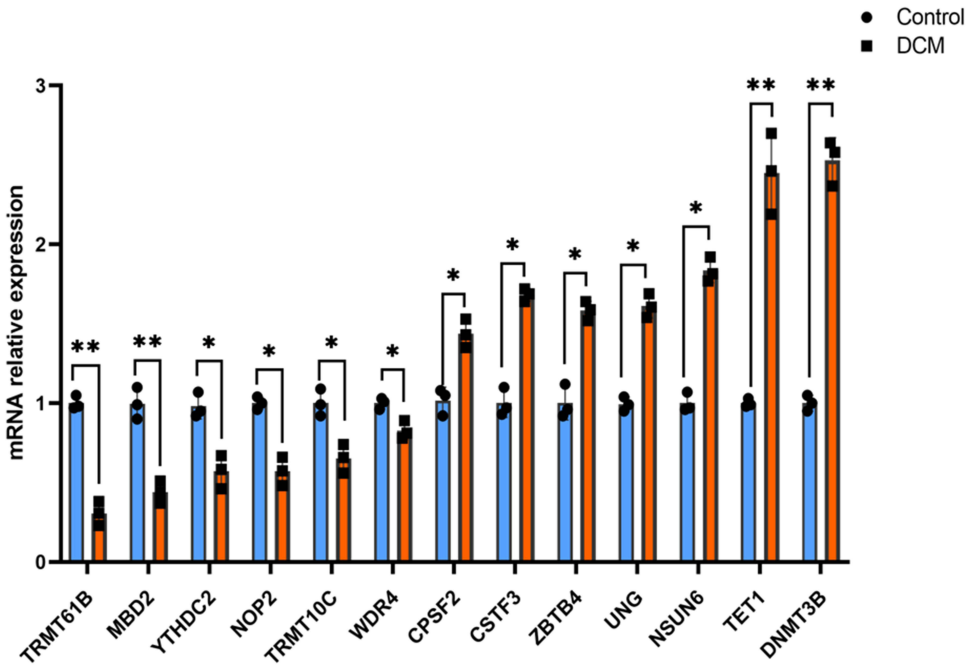

Figure 8 Verification of 13 optimal RNA modification-related genes by qRT-PCR in Control and DCM group. Compared with CTRL group, 0.01<*P<0.05, 0.005<**P<0.01.

modification regulators in DCM or the cardiac remodeling process. This analysis revealed substantial connections among dysregulated RNA modification-related genes, indicating potential interactions among various RNA modifications.

From these dysregulated RNA modification-related genes, 13 genes were identified as diagnostic biomarkers for DCM, including *TRMT61B, MBD2, YTHDC2, NOP2, TRMT10C, WDR4, CPSF2, CSTF3, ZBTB4, UNG, NSUN6, TET1*, and *DNMT3B*. The SVM diagnostic model constructed utilizing these 13 genes demonstrated strong predictive ability for DCM. Mitochondria are essential for structural and functional cardiac remodeling, and their malfunction is associated with heart failure, ventricular hypertrophy, and other cardiac disorders.[19] TRMT61B is mostly localized in the mitochondria and encodes a mitochondria-specific tRNA methyltransferase that catalyzes the formation of m^1A at position 58.[20] Furthermore, TRMT10C is a regulator responsible for m1A in mitochondrial tRNA and mitochondrial ND5 mRNA,[21] and its recessive mutations result in defects in mitochondrial RNA processing.[22] DNMT3B is a major methyltransferase expressed in human and mouse hearts, and its cardiac-specific deletion contributes to myocardial thinning and the progression of severe systolic insufficiency.[23] In addition, the increased expression of DNMT3B and decreased expression of MBD2 have been reported to be involved in epigenetic alterations in ischaemic cardiomyopathy.[24] The potential function of other genes has not been reported in DCM but in various other diseases, such as the predictive value of CPSF2 in papillary thyroid carcinoma[25] and CPSF3 in non-small cell lung cancer,[26] as well as YTHDC2 in acute myocardial infarction.[27]

Analysis of immune infiltration revealed a comparatively significant quantity of naive B cells, M1 macrophages, activated mast cells, and neutrophils in DCM samples. Tang et al discovered that the anomalous distribution of transitional B cells and B1 cells contributed to the etiology of idiopathic DCM. They observed that the proportion of B1 cells was closely linked with DCM severity.[28] Cardiac macrophages are known to modulate adaptive myocardial remodeling, and the reduction of CCR2 macrophages in a DCM mouse model has been associated with increased mortality and impaired ventricular remodeling.[29] Cardiac mast cells are involved in myocardial fibrosis and are considered the core of poor adverse myocardial remodeling.[30,31] The neutrophil/lymphocyte ratio correlates with the severity of DCM and serves as a predictive diagnostic for the condition.[32,33] Additionally, we identified numerous genes (eg, MBD2) that had substantial correlations with infiltrating immune cells in DCM, corroborating prior research. The ablation of MBD2 inhibited TH17 differentiation.[34] In experimental autoimmune myocarditis, MBD2 functioned as a target gene, facilitating pathogenesis and CD4+ T cell immunometabolic dysfunction.[35] Cluster 1 exhibited a superior

https://doi.org/10.2147/JIR.S498496

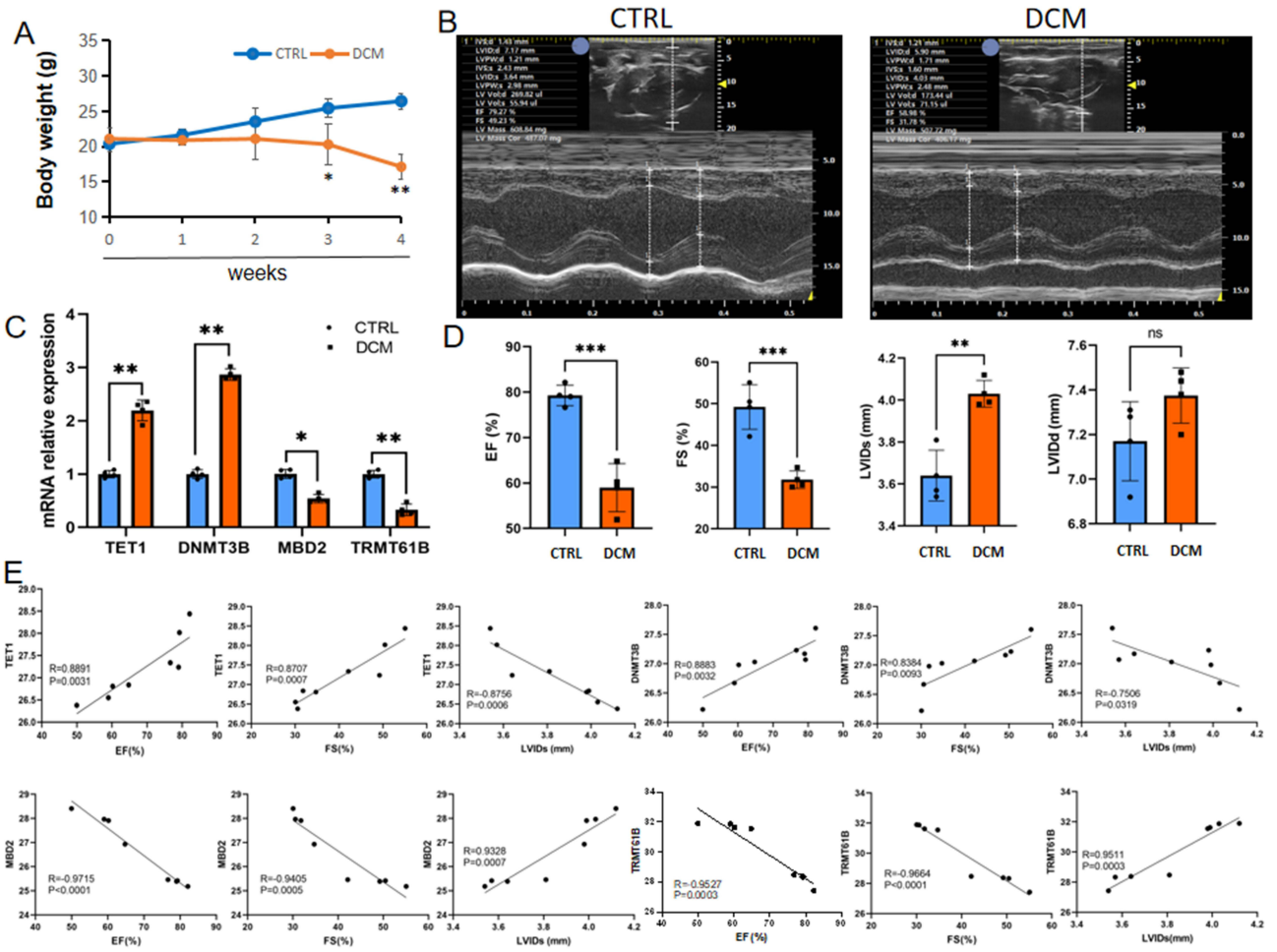

Figure 9 The relationship between *TET1, DNMT3B, MBD2* and *TRMT61B* mRNA levels, and DCM in mice model. (**A**) The body weight in the Control and DCM group. (**B** and **D**) The echocardiography features in the Control and TAAD groups. (**C**) *TET1, DNMT3B, MBD2* and *TRMT61B* mRNA levels in the CTRL and DCM group. (**E**) The correlations between four optimal hub genes *TET1, DNMT3B, MBD2* and *TRMT61B* mRNA levels, and cardiovascular functional parameters in the CTRL and DCM group. Compared with the CTRL group, 0.01<*P<0.05, 0.005<**P<0.01, ***$P<0.005$.

RNA modification score and a worse immune score compared to Cluster 2. Co-stimulatory molecules are important for T-cell activation,[36] and the expression of multiple co-stimulatory molecules has been associated with the development of acute myocarditis and direct myocardial damage in DCM.[37]

We found that various co-stimulatory molecules, including as CD40 and CD27, were dysregulated between the two clusters. Human leukocyte antigens (HLA) are essential genetic markers linked to numerous illnesses, including DCM. The HLA-DR3 antigen has been documented to confer a protective effect in idiopathic DCM,[38] while HLA-DRB1 and HLA-DQB1 gene polymorphism is related to susceptibility to DCM and myocarditis.[39,40] We evaluated the expression of HLA genes between the two molecular clusters and discovered that multiple HLA genes (HLA-DRB1 and HLA-DPB1) were substantially elevated in Cluster 2 compared to Cluster 1. Furthermore, disparities in routes were noted between the two clusters. Cluster 2 exhibited considerable activation of various metabolism-related pathways, whereas Cluster 1 demonstrated activation of primary immunodeficiency and renin-angiotensin system pathways. During heart failure, the renin-angiotensin system (RAS) is activated and is recognized as a significant therapeutic target for the condition.[41] Consequently, RAS gene polymorphism has been regarded as a potential modulator of the phenotypes associated with hypertrophic cardiomyopathy and DCM.[42] Taken together, these findings revealed the significant differences between the two RNA modification- molecular clusters.

In our prior research, we integrated bulk and single-cell RNA sequencing data to discover hub genes of fibroblasts in DCM.[43] In the rat DCM model, we also found that the immune microenvironment around cardiac fibroblasts in

pathological tissue was disordered, and RNA modification could lead to immune microenvironment disorder. Therefore, in order to further study the pathogenesis of DCM, based on the work, we analyzed the application value of RNA modifications related genes in the diagnosis and subtype classification of DCM in this study, and confirmed that RNA-modification-related genes (*TET1, DNMT3B, MBD2* and *TRMT61B*) were most closely associated with decreased cardiac function in DCM. Nevertheless, our research has some limitations. First, because to the considerable heterogeneity exhibited by DCM, further research necessitating a bigger sample size and clinical data will be required. Secondly, there is a lack of linkage among the subtypes, diagnostic genes, and clinical aspects, necessitating more inquiry. The association between the subtypes of RNA modification-related genes and the progression of DCM, along with their functions and processes in the pathological process of DCM, will be further examined.

Conclusions

This work is the inaugural investigation into the systematic role of RNA modification-related genes in DCM. Alongside the established gene signature for DCM, two molecular subtypes of DCM, based on RNA modification-related genes, were discerned; these subtypes exhibited significant variations across multiple dimensions. This study had numerous drawbacks. Initially, over 170 varieties of chemical modifications were recognized on RNAs, and this analysis encompassed just genes associated with many prevalent RNA modifications. The potential functions of genes associated with other RNA modifications in DCM, such as pseudouridine and 2'-O-methylation, were overlooked, despite being prevalent RNA modifications. Secondly, this was a preliminary exploratory study, and several studies should further corroborate the primary findings. The expression and clinical significance of the 13 critical genes, together with the functions of infiltrating immune cells in DCM, are crucial. Furthermore, we successfully produced two distinct RNA modification-related molecular clusters, which exhibited significant differences across various dimensions, demonstrating the viability of RNA modification-based molecular clusters. Nevertheless, it was necessary to examine whether clinical pathological traits varied between the two groups, given the absence of clinical data in the dataset. Dysregulation in the expression patterns of many RNA modification-related genes was noted, leading to the establishment of a diagnostic model based on 13 critical genes for DCM. Two RNA modification molecular clusters with distinct clinical characteristics were subsequently found for DCM. Collectively, this study provides novel insights into the functions of RNA modification in DCM, which may contribute to advances in DCM diagnosis and treatment.

Abbreviations

DCM, Dilated cardiomyopathy; DERMGs, Differentially expressed RNA modification-related genes; LV, left ventricular; GEO, gene expression omnibus; GO, Gene Ontology; KEGG, annotations and Kyoto Encyclopedia of Genes and Genomes; APA, alternative polyadenylation; m^6A, N^6-methyladenosine; m^1A, N^1-methyladenosine; m^5C, 5--methylcytosine; m^7G, N^7-methylguanosine; TTN, Titin; SVM, Support Vector Machine; ROC, receiver operator characteristic.

Data Sharing Statement

These data are publicly available and can be downloaded from the GEO database at no cost.

Ethics Approval

Human data obtained approval from the Ethics Committee of Shaanxi Provincial People's Hospital (No: 2024K-120). All animal use procedures and ethics were reviewed and approved by the Biomedical Ethics Committee of Health Science Center of Xi'an Jiaotong University (No: XJTUAE2023-110). All animal experiments were in accordance with the guide for the care and use of laboratory animals established by United States National Institutes of Health (Bethesda, MD, USA).

Acknowledgments

This work benefited from previous cohort studies. The author sincerely thanks all relevant researchers for the data shared and published.

Funding

This study was supported by Shaanxi Province Innovation Capability Support Plan (2024RS-CXTD-84), Shaanxi Province Health and Gastrointestinal Tumor Organ Precision Diagnosis and Treatment Research Innovation Platform, the Science and Technology Program of Xi'an (23YXYJ0186), and the Basic Natural Science Foundation of Shaanxi Province (2024JC-YBMS-654), Talent funding program of Shaanxi Provincial People's Hospital (2021BJ-07), International Science and Technology Cooperation Program Project of Key Research and Development Plan of Shaanxi Province (2020KWZ-20), the Key Projects of Shaanxi Provincial Department of Education (22JS035).

Disclosure

The authors declare that there is no conflict of interest regarding the publication of this paper.

References

1. Mcgurk KA, Halliday BP. Dilated cardiomyopathy - details make the difference. *Eur J Heart Fail*. 2022;24(7):1197–1199. doi:10.1002/ejhf.2586
2. Weintraub RG, Semsarian C, Macdonald P. Dilated cardiomyopathy. *Lancet*. 2017;390(10092):400–414. doi:10.1016/S0140-6736(16)31713-5
3. Bui QM, Ding J, Hong KN, Adler EA. The genetic evaluation of dilated cardiomyopathy. *Struct Heart*. 2023;7(5):100200. doi:10.1016/j.shj.2023.100200
4. Eldemire R, Mestroni L, Taylor M. Genetics of dilated cardiomyopathy. *Annu Rev Med*. 2024;75(1):417–426. doi:10.1146/annurev-med-052422-020535
5. Mcnally EM, Mestroni L. Dilated cardiomyopathy: genetic determinants and mechanisms. *Circ Res*. 2017;121(7):731–748. doi:10.1161/CIRCRESAHA.116.309396
6. Keating ST, El-Osta A. Metaboloepigenetics in cancer, immunity, and cardiovascular disease. *Cardiovasc Res*. 2023;119(2):357–370. doi:10.1093/cvr/cvac058
7. Yu J, Zeng C, Wang Y. Epigenetics in dilated cardiomyopathy. *Curr Opin Cardiol*. 2019;34(3):260–269. doi:10.1097/HCO.0000000000000616
8. Frye M, Harada BT, Behm M, He C. RNA modifications modulate gene expression during development. *Science*. 2018;361(6409):1346–1349. doi:10.1126/science.aau1646
9. Shi H, Wei J, He C. Where, when, and how: context-dependent functions of RNA methylation writers, readers, and erasers. *Mol Cell*. 2019;74(4):640–650. doi:10.1016/j.molcel.2019.04.025
10. Ju W, Liu K, Ouyang S, Liu Z, He F, Wu J. Changes in n6-methyladenosine modification modulate diabetic cardiomyopathy by reducing myocardial fibrosis and myocyte hypertrophy. *Front Cell Dev Biol*. 2021;9:702579. doi:10.3389/fcell.2021.702579
11. Zhang Z, Zhou K, Han L, et al. RNA m(6)a reader ythdf2 facilitates precursor mir-126 maturation to promote acute myeloid leukemia progression. *Genes Dis*. 2024;11(1):382–396. doi:10.1016/j.gendis.2023.01.016
12. Herman DS, Lam L, Taylor MR, et al. Truncations of titin causing dilated cardiomyopathy. *N Engl J Med*. 2012;366(7):619–628. doi:10.1056/NEJMoa1110186
13. Hinger SA, Wei J, Dorn LE, et al. Remodeling of the m(6)a landscape in the heart reveals few conserved post-transcriptional events underlying cardiomyocyte hypertrophy. *J Mol Cell Cardiol*. 2021;151:46–55. doi:10.1016/j.yjmcc.2020.11.002
14. Dai X, Wang T, Gonzalez G, Wang Y. Identification of yth domain-containing proteins as the readers for n1-methyladenosine in RNA. *Anal Chem*. 2018;90(11):6380–6384. doi:10.1021/acs.analchem.8b01703
15. Choy M, Xue R, Wu Y, Fan W, Dong Y, Liu C. Role of n6-methyladenosine modification in cardiac remodeling. *Front Cardiovasc Med*. 2022;9:774627. doi:10.3389/fcvm.2022.774627
16. Zemlyanskaya EA, Zemlianski V, Pencik A, et al. N6-adenosine methylation of mRNA integrates multilevel auxin response and ground tissue development in Arabidopsis. *Development*. 2023;150(19). doi:10.1242/dev.201775
17. Torrealba N, Aranguiz P, Alonso C, Rothermel BA, Lavandero S. Mitochondria in structural and functional cardiac remodeling. *Adv Exp Med Biol*. 2017;982:277–306. doi:10.1007/978-3-319-55330-6_15
18. Chujo T, Suzuki T. Trmt61b is a methyltransferase responsible for 1-methyladenosine at position 58 of human mitochondrial tRNAs. *RNA*. 2012;18(12):2269–2276. doi:10.1261/RNA.035600.112
19. Safra M, Sas-Chen A, Nir R, et al. The m1a landscape on cytosolic and mitochondrial mRNA at single-base resolution. *Nature*. 2017;551(7679):251–255. doi:10.1038/nature24456
20. Metodiev MD, Thompson K, Alston CL, et al. Recessive mutations in trmt10c cause defects in mitochondrial RNA processing and multiple respiratory chain deficiencies. *Am J Hum Genet*. 2016;98(5):993–1000. doi:10.1016/j.ajhg.2016.03.010
21. Vujic A, Robinson EL, Ito M, et al. Experimental heart failure modelled by the cardiomyocyte-specific loss of an epigenome modifier, dnmt3b. *J Mol Cell Cardiol*. 2015;82:174–183. doi:10.1016/j.yjmcc.2015.03.007
22. Tarazon E, Perez-Carrillo L, Gimenez-Escamilla I, et al. Dnmt3b system dysregulation contributes to the hypomethylated state in ischaemic human hearts. *Biomedicines*. 2022;10(4):866. doi:10.3390/biomedicines10040866
23. Sung TY, Kim M, Kim TY, et al. Negative expression of cpsf2 predicts a poorer clinical outcome in patients with papillary thyroid carcinoma. *Thyroid*. 2015;25(9):1020–1025. doi:10.1089/thy.2015.0079
24. Huang Y, Ji H, Dong J, et al. Cpsf3 promotes pre-mRNA splicing and prevents circrna cyclization in hepatocellular carcinoma. *Cancers*. 2023;15(16):4057. doi:10.3390/cancers15164057
25. Zhang S, Sun S, Zhang Y, Liu J, Wu Y, Zhang X. Comprehensive analysis of n6-methyladenosine RNA methylation regulators in the diagnosis and subtype classification of rheumatoid arthritis. *Biochem Genet*. 2023;2023:1. doi:10.1007/s10528-023-10610-7
26. Tang Q, Cen Z, Lu J, et al. The abnormal distribution of peripheral b1 cells and transition b cells in patients with idiopathic dilated cardiomyopathy: a pilot study. *BMC Cardiovasc Disord*. 2022;22(1):78. doi:10.1186/s12872-022-02461-8

27. Wong NR, Mohan J, Kopecky BJ, et al. Resident cardiac macrophages mediate adaptive myocardial remodeling. *Immunity*. 2021;54(9):2072–2088. doi:10.1016/j.immuni.2021.07.003
28. Palaniyandi SS, Watanabe K, Ma M, Tachikawa H, Kodama M, Aizawa Y. Involvement of mast cells in the development of fibrosis in rats with postmyocarditis dilated cardiomyopathy. *Biol Pharm Bull*. 2005;28(11):2128–2132. doi:10.1248/bpb.28.2128
29. Jin J, Jiang Y, Chakrabarti S, Su Z. Cardiac mast cells: a two-head regulator in cardiac homeostasis and pathogenesis following injury. *Front Immunol*. 2022;13:963444. doi:10.3389/fimmu.2022.963444
30. Avci A, Alizade E, Fidan S, et al. Neutrophil/lymphocyte ratio is related to the severity of idiopathic dilated cardiomyopathy. *Scand Cardiovasc J*. 2014;48(4):202–208. doi:10.3109/14017431.2014.932922
31. Araujo F, Silva R, Oliveira C, Meira Z. Neutrophil-to-lymphocyte ratio used as prognostic factor marker for dilated cardiomyopathy in childhood and adolescence. *Ann Pediatr Cardiol*. 2019;12(1):18–24. doi:10.4103/apc.APC_47_18
32. Zhong J, Yu Q, Yang P, et al. Mbd2 regulates th17 differentiation and experimental autoimmune encephalomyelitis by controlling the homeostasis of t-bet/hlx axis. *J Autoimmun*. 2014;53:95–104. doi:10.1016/j.jaut.2014.05.006
33. Sun P, Wang N, Zhao P, et al. Circulating exosomes control cd4(+) t cell immunometabolic functions via the transfer of mir-142 as a novel mediator in myocarditis. *Mol Ther*. 2020;28(12):2605–2620. doi:10.1016/j.ymthe.2020.08.015
34. Lv X, Zhu S, Wu J, et al. Reciprocal costimulatory molecules control the activation of mucosal type 3 innate lymphoid cells during engagement with b cells. *Cell Mol Immunol*. 2023;20(7):808–819. doi:10.1038/s41423-023-01041-w
35. Seko Y, Ishiyama S, Nishikawa T, et al. Expression of tumor necrosis factor ligand superfamily costimulatory molecules cd27l, cd30l, ox40l and 4-1bbl in the heart of patients with acute myocarditis and dilated cardiomyopathy. *Cardiovasc Pathol*. 2002;11(3):166–170. doi:10.1016/s1054-8807(02)00101-1
36. Jin B, Wu BW, Wen ZC, Shi HM, Zhu J. Hla-dr3 antigen in the resistance to idiopathic dilated cardiomyopathy. *Braz J Med Biol Res*. 2016;49(4):e5131. doi:10.1590/1414-431X20165131
37. Deng J, Luo R, Li X. Hla-drb1 gene polymorphism is associated with idiopathic dilated cardiomyopathy: a meta-analysis. *J Cardiovasc Med*. 2011;12(9):648–652. doi:10.2459/JCM.0b013e328349424b
38. Garnier S, Harakalova M, Weiss S, et al. Genome-wide association analysis in dilated cardiomyopathy reveals two new players in systolic heart failure on chromosomes 3p25.1 and 22q11.23. *Eur Heart J*. 2021;42(20):2000–2011. doi:10.1093/eurheartj/ehab030
39. Januzzi JJ, Ibrahim NE. Renin-angiotensin system blockade in heart failure: more to the picture than meets the eye. *J Am Coll Cardiol*. 2017;69(7):820–822. doi:10.1016/j.jacc.2016.10.083
40. Khan MS, Fonarow GC, Khan H, et al. Renin-angiotensin blockade in heart failure with preserved ejection fraction: a systematic review and meta-analysis. *ESC Heart Fail*. 2017;4(4):402–408. doi:10.1002/ehf2.12204
41. Shao D, Li Y, Wu J, et al. An m6A/m5C/m1A/m7G-Related Long Non-coding RNA Signature to Predict Prognosis and Immune Features of Glioma. *Front Genet*. 2022;13:903117. doi:10.3389/fgene.2022.903117
42. Mei Y, Wang X. RNA modification in mRNA cancer vaccines. *Clin Exper Med*. 2023;23(6):1917–1931. doi:10.1007/s10238-023-01020-5
43. Huang X, Zhao X, Li Y, et al. Combining bulk and single cell RNA-sequencing data to identify hub genes of fibroblasts in dilated cardiomyopathy. *J Inflamm Res*. 2024;17:1. doi:10.2147/JIR.S470860